

Carbon-substitution effect on the electronic properties of MgB₂ single crystals

T. Masui,* S. Lee, and S. Tajima

Superconductivity Research Laboratory, ISTE, 1-10-13 Shinonome, Tokyo 135-0062, Japan

(Received 2 October 2003; revised manuscript received 26 March 2004; published 13 July 2004)

The electronic properties of the carbon-substituted MgB₂ single crystals are reported. The carbon substitution drops T_c below 2 K. In-plane resistivity shows a remarkable increase in residual resistivity by C substitution, while the change of in-plane/out-of-plane Hall coefficients is rather small. Raman scattering spectra indicate that the E_{2g} -phonon frequency radically hardens with increasing the carbon content, suggesting the weakening of electron-phonon coupling. Another striking C effect is the increases of the second critical fields in both in-plane and out-of-plane directions, accompanied by a reduction in the anisotropy ratio. The possible changes in the electronic state and the origin of T_c suppression by C substitution are discussed.

DOI: 10.1103/PhysRevB.70.024504

PACS number(s): 74.70.Ad, 74.25.Fy, 74.25.Gz, 74.25.Dw

I. INTRODUCTION

The electronic properties of MgB₂ have been intensively studied since the discovery of superconductivity in this compound.¹ The band structure of MgB₂ is characterized by the two-dimensional σ bands and the three-dimensional π bands.²⁻⁵ The high superconducting transition temperature (T_c) originates from the strong electron-phonon (e-ph) coupling on the two-dimensional σ bands.⁶⁻⁸ A completely different strength of e-ph coupling in the σ bands and π bands results in two superconducting (SC) gaps. One is a larger gap on the σ bands (Δ_σ) and the other is a smaller one on the π bands (Δ_π).⁹⁻¹⁵ The superconducting state shows a large anisotropy, reflecting mainly the nature of Δ_σ on cylindrical σ bands.^{11,16-21}

Parallel with these studies for understanding a superconductivity mechanism, possibilities to control the electronic properties have been investigated, utilizing pressure, chemical substitution, and irradiation. Among the studies, chemical substitution effect has been one of the hot topics.²²⁻²⁴ Although there are many AlB₂-type compounds, systematic substitution study from MgB₂ is limited to the study of Al substitution for Mg and C substitution for B.²⁵ The primary effect of Al/C substitution is a drop of T_c . We can list the possible sources for the T_c suppression, such as a decrease in density of states, strong interband scattering,²⁶ and the weakening of e-ph coupling. Although electron doping is expected from the valence consideration, the experimentally observed evidence is unclear. Furthermore, the observed decrease in anisotropy ratio of the second critical field (H_{c2}) indicates a substantial change of the electronic state.^{24,27} The C-substitution effect on the two-gap state is also interesting. The recent measurements on polycrystalline samples have revealed the existence of two gaps in the C-substituted MgB₂ with T_c around 20 K,^{24,28,29} which is contrary to the theoretical prediction that the π - and σ -band gaps merge into a single gap giving $T_c=25$ K.²⁶ This fact casts a doubt on the interband scattering scenario. In order to clarify these problems, it is necessary to study more systematically many physical properties using single crystals.

In this paper we try to clarify the carbon-substitution effect on the electronic properties of MgB₂, using a series of

C-substituted single crystals. Electrical resistivity and Raman scattering were measured to investigate the change of disorder effect and/or e-ph coupling. The residual part of in-plane resistivity dramatically increases with increasing carbon content, suggesting the increase of impurity scattering. On the other hand, the change in the slope $d\rho/dT$ is not strong with C content, reflecting the complicated contribution from the multibands. In Raman scattering spectra, the E_{2g} -phonon peak shifts toward higher energy as the carbon content increases, suggesting the weakening of e-ph coupling. The change in carrier density was examined by measuring the Hall coefficient (R_H). The C effect on in-plane/out-of-plane Hall coefficients is weak even in heavily C-substituted crystal, which agrees fairly well with the theoretical calculation within a rigid band scheme. In the superconducting state, the anisotropy ratio decreases with increasing carbon content. The slope of the H_{c2} line (dH_{c2}/dT) increases with C substitution, giving higher H_{c2} in the moderately C-substituted crystals, in both magnetic field directions than that of C-free MgB₂. These changes are explained by the increase of impurity scattering and the modification of band structure by C substitution.

II. EXPERIMENT

Single crystals of MgB₂ were grown under high pressure.³⁰ The carbon-substituted MgB₂ were grown from mixture of Mg, amorphous B and C powders.³¹ Carbon substitution up to 12.5% per boron atom was achieved. Crystals were extracted mechanically from the bulk samples, and well characterized by a four-circle x-ray diffraction technique. The systematic change in the lattice parameter³¹ and the small reliability factor ($R(\leq 3\%)$) obtained in the structure refinement³² prove that C atoms are successfully substituted for B atoms. The C contents were analyzed by an Auger spectroscopy, using the stoichiometric compound MgB₂C₂ as a reference (Fig. 1). The solid line connecting the data point for MgB₂C₂ and the origin is a calibration line for the estimation of C content from the relative C-peak intensity. The plot of relative C-peak intensities versus nominal C content for Mg(B_{1-x}C_x)₂ are well on this line, indicating that the nominal C content almost corresponds to the actual C con-

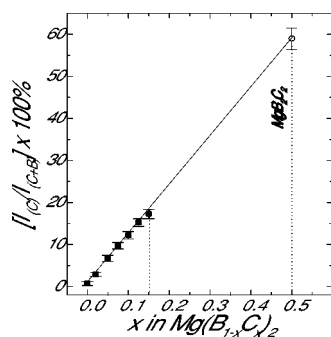


FIG. 1. Average value of relative intensity of the C peak in the Auger spectra as a function of nominal C content x in $\text{Mg}(\text{B}_{1-x}\text{C}_x)_2$. As a reference, the relative intensity of C for MgB_2C_2 is plotted.

tent in $\text{Mg}(\text{B}_{1-x}\text{C}_x)_2$. Resistivity (ρ) was measured by means of a four-probe method. Gold wires were attached to the samples with silver paste. In Hall resistivity measurement, crystals were cut into pieces with a rectangular shape, and gold wires were attached at the side edges of the crystals, in a way similar to resistivity measurement. The contact resistance was less than a few Ohm. In order to extract the R_H components, the samples were rotated 180° in a constant magnetic field. Raman-scattering spectra were measured in the pseudobackscattering configuration with a T64000 Jobin-Yvon triple spectrometer, equipped with a liquid-nitrogen cooled charge-coupled device (CCD) detector. A typical spectral resolution was 3 cm^{-1} . The laser beam with the wavelength of 514.5 nm and the power of $1\text{--}6\text{ mW}$ was focused to a spot of about $0.1 \times 0.1\text{ mm}^2$ on the sample surface. To observe a SC-pair-breaking peak, the crystal was cleaved at room temperature before cooling. For the measurement of phonon peak at room temperature, clean as-grown surfaces were used.

III. RESULTS

The in-plane resistivity (ρ) of $\text{Mg}(\text{B}_{1-x}\text{C}_x)_2$ is shown in Fig. 2. With increasing x , T_c decreases from 38 K for $x=0$

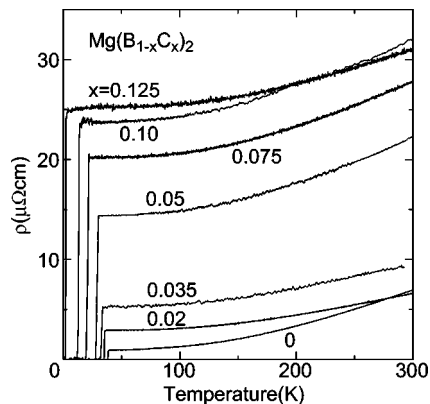


FIG. 2. The temperature dependence of in-plane resistivity of $\text{Mg}(\text{B}_{1-x}\text{C}_x)_2$ single crystals. The T_c s are 38 K, 35 K, 33 K, 30 K, 25 K, 10 K, and 2.0 K for $x=0, 0.02, 0.035, 0.05, 0.075, 0.10,$ and 0.125 crystal, respectively.

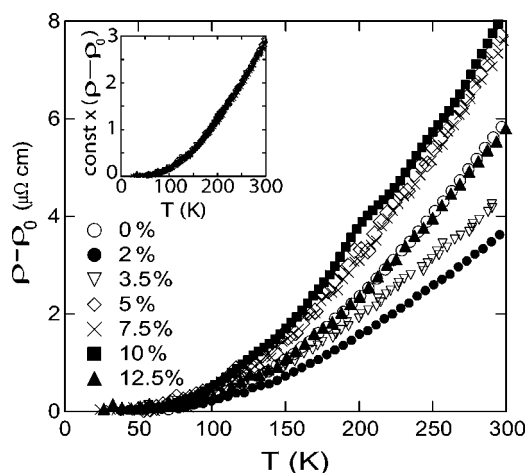


FIG. 3. The temperature-dependent part of in-plane resistivities in Fig. 2, obtained by subtracting the residual part. The inset shows the normalized T -dependent part of the resistivities.

down to 2 K for $x=0.125$. The same T_c values were confirmed by the magnetization measurements for the same batches of crystals.³¹ The most striking effect of C substitution is the increase in residual resistivity (ρ_0). The value of ρ_0 for $x=0.125$ is 25 times larger than that for $x=0$, which indicates a remarkable increase of carrier scattering rate due to impurity. Since an increase in ρ_0 leads to a decrease in residual resistivity ratio (r.r.r.), the result can be presented as a decrease in r.r.r. with increasing x . The empirical correlation between r.r.r. and T_c in various MgB_2 samples has been reported from the very beginning of the MgB_2 study,³³ although there is no theoretical background to consider r.r.r. as a parameter determining T_c in an s -wave Bardeen-Cooper-Schrieffer (BCS) superconductor. It is demonstrated in Fig. 2 that the physical meaning of r.r.r. reduction is the increase in ρ_0 , and that the correlation between r.r.r. and T_c can be discussed in terms of the correlation between ρ_0 and T_c .

In contrast to the dramatic increase in ρ_0 , the change in resistivity slope (dp/dT) is not pronounced. Figure 3 plots the resistivity curves after subtracting residual resistivity. Looking at the data carefully, one may find a slight decrease in the slope (dp/dT) at $x=0.02$ and 0.035 . Similar change was observed in the MgB_2 single crystals with slightly different T_c .³⁴ The decrease in slope results in the cross touch of the two curves for $x=0$ and 0.02 at the high temperature in Fig. 2, which is reproducible and thus intrinsic. Since both of the σ and π bands contribute to the in-plane conduction, the interpretation of the change in $\rho(T)$ is complicated. The decrease of dp/dT at low C contents followed by the recovery of the slope at higher C contents does not allow a simple interpretation in terms of the change in e-ph coupling constant or plasma frequency within a one-band picture. It may be possible that the relative weight of σ - and π -band contribution change with C substitution through the change in scattering rate and plasma frequency in each band.

As demonstrated in the inset of Fig. 3, all the T -dependent parts of in-plane resistivity are scaled well. The almost unchanged $\rho(T)$ profile shown in the inset of Fig. 3 implies that $\rho(T)$ below 300 K is less sensitive to the change in Debye

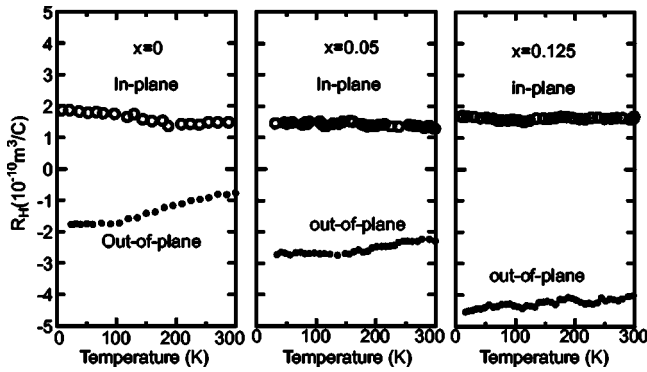


FIG. 4. Hall coefficient for C-substituted MgB_2 . In-plane R_H was measured in $H//c$, $I//ab$. Out-of-plane R_H was measured in $H//ab$, $I//ab$, $I \perp H$. The out-of-plane R_H for $x=0$ sample was replotted from Ref. 5.

temperature, because the T -linear temperature region gives a rough estimate of Debye temperature. The high-temperature slope of resistivity was previously discussed as a measure of e-ph coupling, assuming that σ -band carriers dominate in-plane conduction.³⁵ However, the present result indicates that this is an oversimplified picture and that the π -band contribution must be taken into account.

The change of carrier concentration by C substitution was expected from the valence consideration, and it should affect the R_H s. In Fig. 4 the in-plane and out-of-plane Hall coefficients (R_H) are presented. In all the samples the in-plane R_H s are positive and the out-of-plane R_H s are negative. Although quantitative analysis of R_H is difficult in a multi-band system, the negative sign of out-of-plane R_H reflects the dominant contribution of the π -band electrons to the c -axis conduction, while the positive R_H indicates the contribution of the σ -band holes to the in-plane conduction.⁵ The results in Fig. 4 demonstrate that this two-carrier picture still holds even in heavily C-substituted MgB_2 .

As for the in-plane direction, the value of R_H does not change so much, while the absolute value of out-of-plane R_H increases with increasing carbon content. In a simple free-carrier model, the increase of the absolute value of out-of-plane R_H implies the decrease of electron carrier density, which is contrary to the expectation of electron doping. However, since the value of R_H is determined by the sum of each contribution from σ or π bands, it should be carefully interpreted. The decrease in the π -band hole contribution might substantially affect the out-of-plane R_H in this case. It should be noted that the calculation within a rigid-band scheme³⁶ predicts the almost constant in-plane R_H and the enhanced out-of-plane R_H as a function of additional electron density. The present results follow the same tendency of changes in R_H 's, although the absolute values of R_H 's are one order larger than the calculated ones. The origin of the discrepancy between experiment and the rigid-band calculation is not clear.

Figure 5 illustrates the Raman-scattering spectra for $x=0$, 0.05, and 0.125. With increasing x , the E_{2g} -phonon peak shows hardening. In the C-free MgB_2 , the E_{2g} -phonon peak is extremely softened owing to the strong coupling with the σ bands. The increase of the E_{2g} -peak energy suggests the

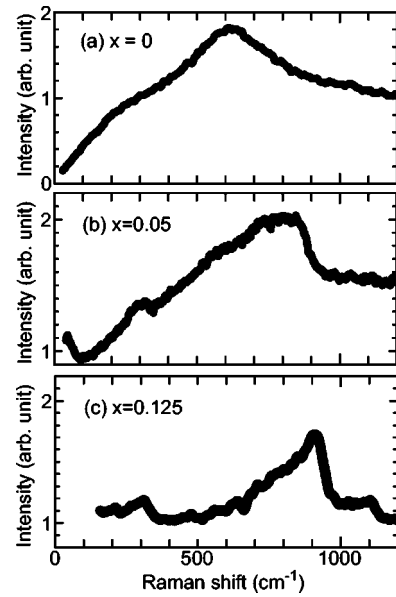


FIG. 5. The polarized in-plane Raman scattering spectra of $\text{Mg}(\text{B}_{1-x}\text{C}_x)$ at room temperature for (a) $x=0$ (replotted from Ref. 39), (b) $x=0.05$, and (c) $x=0.125$.

weakening of e-ph coupling by C substitution. The narrowing of the peak width is more evidence for the weakening of e-ph coupling. A similar observation was reported in Al-substituted MgB_2 .^{37,38} The lineshape of the E_{2g} peak for C-substituted MgB_2 becomes asymmetric probably because of a distribution of the peak energy due to the disorder and inhomogeneity induced by C substitution. The effect of inhomogeneous C distribution may be seen in the relatively less reproducible $\rho(T)$ data for high C content, $x \geq 0.10$. C substitution also creates another peak at around 300 cm^{-1} that may originate from the disorder.

To observe a SC gap, low-temperature Raman spectra were measured. In Fig. 6, the spectra for $x=0$ and $x=0.02$ are presented. In the spectra of $x=0$ crystal, a sharp pair-breaking peak manifests itself at $\sim 100 \text{ cm}^{-1}$ below T_c .^{39,40} On the other hand, for $x=0.02$ crystal, redistribution of low-

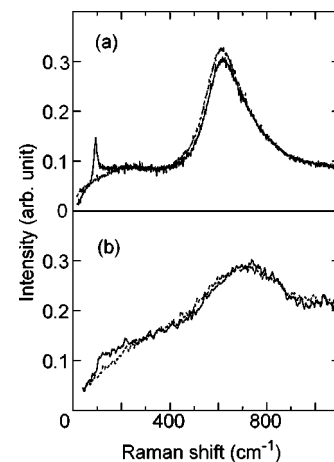


FIG. 6. The depolarized in-plane Raman scattering spectra (a) for $x=0$ at 40 K (dotted line) and 15 K (solid line) (Ref. 39) and (b) for $x=0.02$ at 40 K (dotted line) and 10 K (solid line).

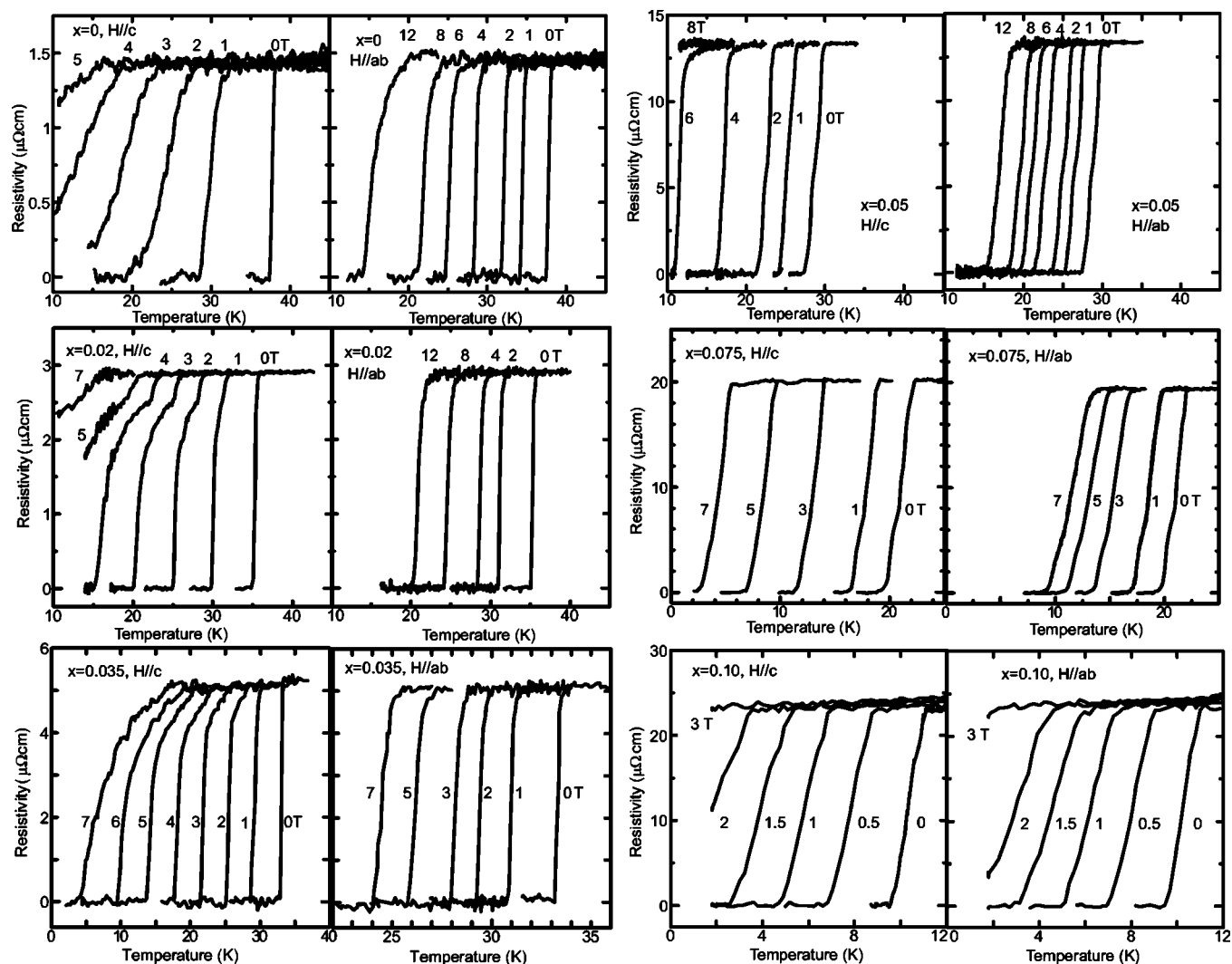


FIG. 7. The SC transition behavior of resistivity for $\text{Mg}(\text{B}_{1-x}\text{C}_x)_2$ single crystals with $x=0, 0.02, 0.035, 0.05, 0.075,$ and 0.10 in $H//c$ and $H//ab$.

energy electronic continuum is observed below T_c , whereas a pair-breaking peak is almost suppressed. At higher C content, the redistribution of electronic continuum below T_c becomes undetectable.

To explain the suppression of the pair-breaking peaks, two possibilities may be pointed out. The first is that the inhomogeneity induced by C substitution leads to a distribution of SC gap in the crystal, which causes a spread of SC-gap peaks. The second is the strong impurity scattering that is seen as a remarkable increase in residual resistivity shown in Fig. 2. The scattering rate $1/\tau$ is roughly estimated to be $\sim 90 \text{ cm}^{-1}$ for $x=0.02$, using $1/\tau=30 \text{ cm}^{-1}$ for pure MgB_2 and $\rho_0(x=0.02)/\rho_0(x=0, \text{pure}) \sim 3$. This $1/\tau$ value is comparable to the gap energy $2\Delta (\sim 100 \text{ cm}^{-1})$. It means that the system changes into a dirty limit regime, in which a gap feature in the Raman spectra is smeared out as is typically seen in the c -axis Raman spectrum of MgB_2 .¹³

C substitution also modifies superconducting state properties. Figure 7 shows the resistivities near T_c in magnetic fields. Although the T_c at $H=0$ decreases by C substitution,

the reduction of T_c by magnetic field becomes small in the C-substituted crystals. For example, the magnetic field suppressing T_c below 10 K is higher for $x=0.05$ than for $x=0$ in $H//c$, while in $H//ab$ T_c at $H=12 \text{ T}$ is nearly the same for $x=0$ and 0.05 in spite of the 10 K difference at $H=0$. The anisotropy also decreases by C substitution, and eventually disappears at $x=0.10$. In the crystal with $x=0.10$, the transition behavior is almost independent of field direction. The weakening of the resistivity transition broadening that is evident in $H//c$ also suggests the increase of three-dimensional nature by C substitution. For $x=0.10$, SC transitions show nearly parallel shifts by applying magnetic fields.

The temperature dependence of critical magnetic field $H_c^{\rho=0}$, determined by zero resistivity temperature, is plotted in Fig. 8. Here, we regard $H_c^{\rho=0}$ as a measure of H_{c2} , although the definition of H_{c2} is controversial.^{41,42} With increasing x , the slope $dH_c^{\rho=0}/dT$ increases in both field directions. As a result of steep increase in the slope, $H_c^{\rho=0}$ at $T=0$ increases by C substitution in both field directions, in spite of the T_c suppression. This is consistent with the tendency in previous

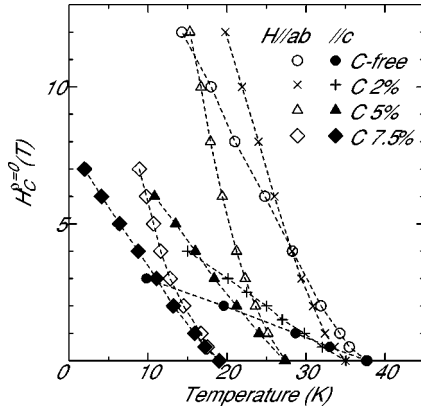


FIG. 8. H-T phase diagram for $\text{Mg}(\text{B}_{1-x}\text{C}_x)_2$, determined from the zero-resistivity temperature. Lines are guides for the eyes.

polycrystal studies^{24,43,44} and in our single crystal MgB_2 with slightly different T_c .³⁴ It was found by the torque measurement that the enhanced $H_c^{p=0}$ reaches 33 T at $T \approx 0$ K for $x = 0.05$.⁴⁵ In Fig. 9, the coherence lengths ξ_{ab} and ξ_c estimated from the slope in Fig. 8 and the anisotropy ratio ξ_{ab}/ξ_c are plotted. To take into account the transition broadening in resistivity, we also plot the critical fields determined by the midpoint of resistive transition as open symbols. It is indicated that the C substitution decreases anisotropy, even if the uncertainty of H_{c2} 's is taken into account. Almost isotropic superconductivity is observed above 10%. At the low C contents below $x=0.075$, the decrease of anisotropy ratio is caused by the shrink of ξ_{ab} predominantly due to the shortening of the in-plane mean free path. In heavily C-substituted crystal, both ξ_{ab} and ξ_c are elongated.

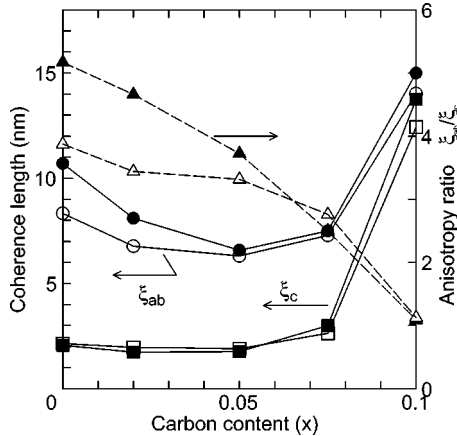


FIG. 9. Coherence lengths estimated by the WHH (Werthamer, Helfand, Hoenberg) formula, $H_{c2}(0 \text{ K}, H//c) = \phi_0 / (2\pi\xi_{ab}^2) = 0.7(dH_{c2}/dT) \times T_c$ and $H_{c2}(0 \text{ K}, H//ab) = \phi_0 / (2\pi\xi_{ab}\xi_c) = 0.7(dH_{c2}/dT) \times T_c$ (Ref. 46). Here the lower-temperature slope is used to avoid the smaller-gap contribution. The circles and squares represent ξ_{ab} and ξ_c , respectively. The triangles represent anisotropy ratios ξ_{ab}/ξ_c . The closed symbols are estimated from zero-resistivity temperature. The open symbols are estimated from the midtemperatures of the SC transition.

IV. DISCUSSION

The most remarkable effect of C substitution in MgB_2 is the decrease of T_c . Since the high-temperature superconductivity of MgB_2 originates from the strong e-ph coupling in σ bands, it is natural to ascribe the origin of decreasing T_c to the change of σ -band properties. The two changes in the σ -band electronic state can be considered. One is the band filling, i.e., the shift of the Fermi level, which decreases the hole density of states $N^\sigma(\epsilon_F)$ and shrinks the cylindrical Fermi surface. The other change is the increase of carrier scattering rate. It is hard to detect the change of $N^\sigma(\epsilon_F)$ selectively. Resistivity and Hall coefficient are affected by both of the σ and π bands, although they show anisotropy. In the present study, the change of $N^\sigma(\epsilon_F)$ can be seen in the weakening of e-ph coupling, because the $N(\epsilon_F)$ is one of the parameters that determines the coupling constant λ .⁶ The suppression of e-ph coupling is clearly observed as the pronounced hardening and narrowing of the E_{2g} phonon in Raman-scattering spectra in Fig. 5. The change of the σ -band Fermi surface would also reduce the e-ph coupling via the change of deformation potential. We note that the shift of E_{2g} -phonon frequency is stronger than the moderate change in $N^\sigma(\epsilon_F)$ at low C contents. The observed decrease of T_c is not monotonous, but the smooth change becomes steeper as the substitution proceeds. This change in T_c -suppression rate seems to be related to the calculated drop of $N(\epsilon_F)$ by electron doping.⁶ The band calculation predicts that superconductivity will be suppressed by ~ 0.25 electron doping per unit cell.^{6,47} The nearly suppressed $T_c \sim 2$ K at $x=0.125$ in our study roughly corresponds to this critical doping.

Another factor that should be discussed as an origin of decreasing T_c is the strong interband scattering²⁶ that is related to the large increase of residual resistivity. When strong scattering is introduced, the two-gap SC picture is no longer valid, and isotropic superconductivity with a single SC gap is realized. As for C-substituted MgB_2 , the studies on polycrystalline samples have revealed that the two SC gaps survive even in the sample with $T_c \sim 20$ K.^{24,28,29} It should be noted that the estimated T_c for a dirty-limit is about 20 K without change in $N(\epsilon_F)$. Therefore, it is unlikely that the interband scattering is the primary origin of decreasing T_c for $x \leq 0.075$. At higher C content $x \geq 0.10$, on the other hand, the interband scattering may play some role. In such highly C-substituted crystal, the superconductivity becomes almost isotropic, although the anisotropic band structure is still suggested by the anisotropy of Hall coefficients for $x=0.125$. In order to explain the isotropic superconductivity with the anisotropic band structure, the strong interband scattering scenario is preferable. Interband scattering may be enhanced by induced disorder by C substitution, such as buckling of the B planes. Accordingly, we conclude that both the decrease in λ and the increase in interband scattering rate contribute to the decrease in T_c , although the degree of contribution changes as a function of x .

In order to extract the change of the σ bands, the critical field H_{c2} provides useful information, because it is predominantly determined by the σ -band gap at $H \geq 0.5 T$.¹¹ The increase of $H_c^{p=0}$ is due to the increase of impurity scattering

via the shortening of ξ , as is expected from the relation $\xi^{-1} \simeq \xi_0^{-1} + l^{-1}$, where ξ_0 is coherence length in clean limit, and l is mean free path. The radical decrease of l was clearly seen in Fig. 2 as an increase of residual resistivity. At $x=0.05$, for example, the l is one order shorter than that for $x=0$, which results in the relation $l \sim \xi$. The validity of dirty-limit picture was also demonstrated as the smearing of pair-breaking peak in the Raman spectrum (Fig. 6).

The anisotropy change in $H_c^{\rho=0}$ can be explained by the anisotropic change of ξ . As seen in Fig. 9, the anisotropy decrease is mainly due to the rapid shrink of ξ_{ab} . This indicates that the scattering rate for the σ -band carriers increases in an anisotropic way. Since the C substitution of atoms takes place on B planes, it is likely that the introduced disorder primarily affects the σ -band conduction along the B planes. In the heavily C-substituted crystals, where the remarkable decrease in Δ elongates ξ , interband scattering may additionally contribute to the isotropic SC state, as observed in the crystal with $x=0.10$ and 0.125 .

V. SUMMARY

We have presented the electronic properties of carbon-substituted MgB_2 single crystals. The effects of C substitu-

tion are twofold. One is the increase of impurity scattering, and the other is the band filling that reduces $N_\sigma(\epsilon_F)$ and modifies the shape of the Fermi surface. The former increases rapidly the residual resistivity, enhances the critical magnetic fields, and smears out the pair-breaking peak in Raman spectra. A predominant effect of the latter is the shift of the E_{2g} peak, suggesting the weakening of e-ph coupling by C substitution. This is the primary reason for the decrease of T_c . The theoretically expected tendency of the electron-doping effect on R_H was confirmed, but the difference of the absolute values still remains to be solved.

ACKNOWLEDGMENTS

One of the authors (T.M.) thanks Professor P. C. Canfield and Professor W. E. Pickett for their helpful comments. T.M. is supported by the JSPS. This work is supported by New Energy and Industrial Technology Development Organization (NEDO) as Collaborative Research and Development of Fundamental Technologies for Superconductivity Applications.

*Electronic address: masui@istec.or.jp

- ¹J. Nagamatsu, N. Nakagawa, T. Muranaka, Y. Zenitani, and J. Akimitsu, *Nature (London)* **410**, 63 (2001).
- ²J. Kortus, I. I. Mazin, K. D. Belashchenko, V. P. Antropov, and L. L. Boyer, *Phys. Rev. Lett.* **86**, 4656 (2001).
- ³H. Uchiyama, K. M. Shen, S. Lee, A. Damascelli, D. H. Lu, D. L. Feng, Z.-X. Shen, and S. Tajima, *Phys. Rev. Lett.* **88**, 157002 (2002).
- ⁴E. A. Yelland, J. R. Cooper, A. Carrington, N. E. Hussey, P. J. Meeson, S. Lee, A. Yamamoto, and S. Tajima, *Phys. Rev. Lett.* **88**, 217002 (2002).
- ⁵Yu. Eltsev, K. Nakao, S. Lee, T. Masui, N. Chikumoto, S. Tajima, N. Koshizuka, and M. Murakami, *Phys. Rev. B* **66**, 180504(R) (2002).
- ⁶J. M. An and W. E. Pickett, *Phys. Rev. Lett.* **86**, 4366 (2001).
- ⁷Hyoung Joon Choi, David Roundy, Hong Sun, Marvin L. Cohen, and Steven G. Louie, *Phys. Rev. B* **66**, 020513(R) (2002); *Nature (London)* **418**, 758 (2002).
- ⁸A. A. Golubov, J. Kortus, O. V. Dolgov, O. Jepsen, Y. Kong, O. K. Andersen, B. J. Gibson, K. Ahn, and R. K. Kremer, *J. Phys.: Condens. Matter* **14**, 1353 (2002).
- ⁹Y. Wang, T. Plackowski, and A. Junod, *Physica C* **355**, 179 (2001).
- ¹⁰F. Bouquet, R. A. Fisher, N. E. Phillips, D. G. Hinks, and J. D. Jorgensen, *Phys. Rev. Lett.* **87**, 047001 (2001).
- ¹¹F. Bouquet, Y. Wang, I. Sheikin, T. Plackowski, and A. Junod, S. Lee, and S. Tajima, *Phys. Rev. Lett.* **89**, 257001 (2002).
- ¹²S. Tsuda, T. Yokoya, T. Kiss, Y. Takano, K. Togano, H. Kito, H. Ihara, and S. Shin, *Phys. Rev. Lett.* **87**, 177006 (2001).
- ¹³J. W. Quilty, S. Lee, S. Tajima, and A. Yamanaka, *Phys. Rev. Lett.* **90**, 207006 (2003).
- ¹⁴S. Souma, Y. Machida, T. Sato, T. Takahashi, H. Matsui, S.-C. Wang, H. Ding, A. Kaminski, J. C. Campuzano, S. Sasaki, and K. Kadowaki, *Nature (London)* **423**, 65 (2003).
- ¹⁵S. Tsuda, T. Yokoya, Y. Takano, H. Kito, A. Matsushita, F. Yin, H. Harima, and S. Shin, *Phys. Rev. Lett.* **91**, 127001 (2003).
- ¹⁶F. Simon, A. Jánossy, T. Fehér, F. Murányi, S. Garaj, L. Forró, C. Petrovic, S. L. Bud'ko, G. Lapertot, V. G. Kogan, and P. C. Canfield, *Phys. Rev. Lett.* **87**, 047002 (2001).
- ¹⁷Yu. Eltsev, S. Lee, K. Nakao, N. Chikumoto, S. Tajima, N. Koshizuka, and M. Murakami, *Phys. Rev. B* **65**, 140501(R) (2001).
- ¹⁸M. Xu, H. Kitazawa, Y. Takano, J. Ye, K. Nishida, H. Abe, A. Matsushita, and G. Kido, *Appl. Phys. Lett.* **79**, 2779 (2001).
- ¹⁹K. H. P. Kim, J. H. Choi, C. U. Jung, P. Chowdhury, Hyun-Sook Lee, M. S. Park, H. J. Kim, J. Y. Kim, Z. Du, E. M. Choi, M. S. Kim, W. N. Kang, S. I. Lee, G. Y. Sung, and J. Y. Lee, *Phys. Rev. B* **65**, 100510(R) (2002).
- ²⁰A. K. Pradhan, Z. X. Shi, M. Tokunaga, T. Tamegai, Y. Takano, K. Togano, H. Kito, and H. Ihara, *Phys. Rev. B* **64**, 212509 (2001).
- ²¹A. V. Sologubenko, J. Jun, S. M. Kazakov, J. Karpinski, H. R. Ott, *cond-mat/0111273* (2001).
- ²²J. S. Slusky, N. Rogado, K. A. Regan, M. A. Hayward, P. Khalifah, T. He, K. Inumaru, S. M. Loureiro, M. K. Haas, H. W. Zandbergen, and R. J. Cava, *Nature (London)* **410**, 343 (2001).
- ²³T. Takenobu, T. Ito, D. H. Chi, K. Prassides, and Y. Iwasa, *Phys. Rev. B* **64**, 134513 (2001).
- ²⁴R. A. Ribeiro, S. L. Bud'ko, C. Petrovic, and P. C. Canfield, *Physica C* **384**, 227 (2003).
- ²⁵R. J. Cava, H. W. Zandbergen, and K. Inumaru, *Physica C* **385**, 8 (2003).
- ²⁶A. Y. Liu, I. I. Mazin, and J. Kortus, *Phys. Rev. Lett.* **87**, 087005 (2001).
- ²⁷M. Pissas, G. Papavassiliou, M. Karayanni, M. Fardis, I. Maurin,

- I. Margiolaki, K. Prassides, and C. Christides, *Phys. Rev. B* **65**, 184514 (2002).
- ²⁸P. Samuely, Z. Hoľanová, P. Szabó, J. Kačmarčík, R. A. Ribeiro, S. L. Bud'ko, and P. C. Canfield, *Phys. Rev. B* **68**, 020505(R) (2003).
- ²⁹H. Schmidt, K. E. Gray, D. G. Hinks, J. F. Zasadzinski, M. Avdeev, J. D. Jorgensen, and J. C. Burley, *Phys. Rev. B* **68**, 060508(R) (2003).
- ³⁰S. Lee, H. Mori, T. Masui, Y. Eltsev, A. Yamamoto, and S. Tajima, *J. Phys. Soc. Jpn.* **70**, 2255 (2001).
- ³¹S. Lee, T. Masui, A. Yamamoto, H. Uchiyama, and S. Tajima, *Physica C* **397**, 7 (2003).
- ³²A. Yamamoto and S. Lee, private communication.
- ³³C. Buzea and T. Yamashita, *Supercond. Sci. Technol.* **14**, R115 (2001).
- ³⁴T. Masui, S. Lee, and S. Tajima, *Physica C* **392-396**, 281 (2003).
- ³⁵T. Masui, K. Yoshida, S. Lee, A. Yamamoto, and S. Tajima, *Phys. Rev. B* **65**, 214513 (2002).
- ³⁶G. Satta, G. Profeta, F. Bernardini, A. Continenza, and S. Massidda, *Phys. Rev. B* **64**, 104507 (2001).
- ³⁷B. Renker, K. B. Bohnen, R. Heid, D. Ernst, H. Schober, M. Koza, P. Adelman, P. Schweiss, and T. Wolf, *Phys. Rev. Lett.* **88**, 067001 (2002).
- ³⁸P. Postorino, A. Congeduti, P. Dore, A. Nucara, A. Bianconi, D. Di Castro, S. De Negri, and A. Saccone, *Phys. Rev. B* **65**, 020507 (2001).
- ³⁹J. W. Quilty, S. Lee, A. Yamamoto, and S. Tajima, *Physica C* **378-381**, 38 (2002).
- ⁴⁰J. W. Quilty, S. Lee, A. Yamamoto, and S. Tajima, *Phys. Rev. Lett.* **88**, 087001 (2002).
- ⁴¹U. Welp, A. Rydh, G. Karapetrov, W. K. Kwok, G. W. Crabtree, C. Marcenat, L. M. Paulius, L. Lyard, T. Klein, J. Marcus, S. Blanchard, P. Samuely, P. Szabo, A. G. M. Jansen, K. H. P. Kim, C. U. Jung, H.-S. Lee, B. Kang, and S.-I. Lee, *Physica C* **385**, 154 (2003).
- ⁴²T. Masui, S. Lee, and S. Tajima, *Physica C* **383**, 299 (2003).
- ⁴³C. H. Cheng, H. Zhang, Y. Zhao, Y. Feng, X. F. Rui, P. Munroe, H. M. Zeng, N. Koshizuka, M. Murakami, *Supercond. Sci. Technol.* **16**, 1182 (2003).
- ⁴⁴S. Soltanian, J. Horvat, X. L. Wang, P. Munroe, and S. X. Dou, *Physica C* **390**, 185 (2003).
- ⁴⁵E. Ohmichi, T. Masui, S. Lee, S. Tajima, and T. Osada, *J. Phys. Soc. Jpn.* (to be published).
- ⁴⁶N. R. Werthamer, N. Helfand, and P. C. Hohenberg, *Phys. Rev.* **147**, 295 (1966).
- ⁴⁷N. I. Medvedeva, A. L. Ivanovskii, J. E. Medvedeva, and A. J. Freeman, *Phys. Rev. B* **64**, 020502(R) (2001).